SCIENTIFIC REPORTS

OPEN

SUBJECT AREAS:
ELECTRONIC MATERIALS
CHEMICAL PHYSICS
MOLECULAR ELECTRONICS
ELECTRONIC DEVICES

Received
20 November 2013

Accepted
18 July 2014

Published
15 September 2014

Correspondence and requests for materials should be addressed to R.-Q.Z. (aprqz@cityu.edu.hk)

Rectifying Properties of Oligo(Phenylene Ethynylene) Heterometallic Molecular Junctions: Molecular Length and Side Group Effects

Xiao-Xiao Fu[1,2], Rui-Qin Zhang[1,3], Guang-Ping Zhang[2] & Zong-Liang Li[2]

[1]Beijing Computational Science Research Center, Beijing 100084, P. R. China, [2]College of Physics and Electronics, Shandong Normal University, Ji'nan 250014, P. R. China, [3]Department of Physics and Materials Science, City University of Hong Kong, Hong Kong SAR, P. R. China.

The rectifying properties of α,ω-dithiol terminated oligo(phenylene ethynylene) molecules sandwiched between heterometallic electrodes, including the molecular length and side group effects, are theoretically investigated using the fully self-consistent nonequilibrium Green's function method combined with density functional theory. The results show nonlinear variation with changes in molecule length: when the molecule becomes longer, the current decreases at first and then increases while the rectification shifts in the opposite direction. This stems from the change in molecular eigenstates and the coupling between the molecule and electrodes caused by different molecular lengths. The rectifying behavior of heterometallic molecular junctions can be attributed to the asymmetric molecule-electrode contacts, which lead to asymmetric electronic tunneling spectra, molecular eigenvalues, molecular orbitals, and potential drop at reversed equivalent bias voltages. Our results provide a fundamental understanding of the rectification of heterometallic molecular junction, and a prediction of rectifiers with different rectification properties from those in the experiment, using electrodes with reduced sizes.

The molecular diode is one of the most important electronic components in use, and has attracted considerable attention since the advent of molecular electronics[1–3]. It is used for molecular logic circuits and memory elements. Since Aviram and Ratner proposed the first prototype in 1974[1], considerable efforts have been made to identify molecular junctions with rectifying properties[4–10]. The molecular junctions of asymmetric structures introduced by asymmetric molecules and molecule-electrode contacts may demonstrate rectifying behavior. The asymmetric molecules contain D-σ-A, D-π-A, and D-A types, which consist of a donor and an accepter molecular fragment with an σ, π, and no bridge, respectively. Asymmetric molecule-electrode contacts include asymmetric terminal anchoring groups, molecule-electrode contact configurations, and electrode materials. It has been found that the rectifying properties of devices can be fine-tuned by changing the molecular length[11,12], terminal anchoring groups[13–15], side groups[12], molecule-electrode contact configurations[16–18], the acid-base property of the solution[7,19,20], and the external potential field[21].

However, most studies are based on molecular junctions with monometallic electrodes. It is rare for research attention to be paid to structures incorporating heterometallic electrodes. In 2003, the asymmetric electrode pairs with nanometer separation made of two distinct metals were fabricated for the first time, using the method involving the electrodeposition of a second metal on a pre-existing lithographically defined electrode. Its utility was demonstrated by making single-electron tunneling devices incorporating 2-nm gold nanocrystals[22]. In 2009, heterometallic nanogaps for molecular transport junctions were manufactured by Chen et al, based upon on-wire lithography technique, which chemically enables to synthesize a wide variety of nanowire-based structures[23]. Furthermore, they demonstrated that the molecular transport junctions consisting of a thiol-terminated oligo (phenylene ethynylene) (OPE) molecule assembled into heterometallic nanogaps exhibit molecular diode behavior. Recently, molecular junctions with asymmetric metallic electrodes have stimulated the interest of theoreticians, who have conducted several investigations of the topic. In 2011, Pan et al. paired an Au electrode with, respectively, Li, Pb, Ag electrodes sandwiching an OPE molecule to fabricate molecular junctions and study the current rectification induced by asymmetrical electrodes[24]. In 2012, Liu et al. investigated the effect of different

electrodes on the Fano resonance of molecular devices composed of π-conjugated molecules anchored between Au and Ag electrodes[25]. Nevertheless, existing theoretical work does not provide a convincing explanation of Chen's experimental reports[23]. Although Pan et al. give a reasonable explanation of the rectification caused by asymmetrical electrodes[24], their OPE molecule is different from that reported by Chen. The OPE molecule in Pan's research contains 3 benzene rings while that in Chen's experiment consists of 5 benzene rings with side groups. The effect of molecular length and side group on the rectification of heterometallic molecular junctions is still unknown. Consequently, the mechanism of the rectifying properties of heterometallic molecular junctions still needs to be comprehensively understood.

This work presents a theoretical study of the current rectification of the heterometallic molecular junctions of OPE molecules sandwiched between Pt and Au electrodes based on calculations using density functional theory and nonequilibrium Green's function method. The rectifying behavior is studied with focus on the effect of molecular length and side group. The underlying principles of the rectifying properties of asymmetric electrodes are ascertained from the electronic tunneling spectra, molecular orbitals, eigenvalue evolutions, and potential drop of the system.

Results

As stated above, the study of the rectification of the OPE heterometallic molecular junctions includes two aspects, the molecular length and side group effects. In the first study, OPE molecules containing 2–6 benzene rings (n = 2 : 6) with Au as the left electrode and Pt as the right electrode are chosen to investigate the molecular length effect on the rectification of heterometallic molecular junctions, as shown in Figure 1(a). The OPE molecules illustrated in Figure 1(b), containing 5 benzene rings, are used to study the side group effect. Two kinds of molecules are considered here; one is with ethyl (Et) side groups and the other without side groups for the purpose of comparison. Given these two types of molecules, three electronic transport models are considered here, denoted by M1, M2, and M3. In M1, the OPE molecule with Et side groups connects the left Pt and the right Au electrode, as is used in the experiment. M2 is constructed by exchanging the orientation of the molecule in M1, and in M3 the molecular core is replaced by one with no side group. In each of those models, the molecule anchors the electrodes through the thiol groups at the hollow positions of (111) metal surfaces.

Molecular length effect. The current through each of the optimized molecular junctions (n = 2 : 6) is calculated in the bias range of [−1.0 V, 1.0 V] (see Figure 2(a)). The asymmetry of the current-voltage (*I-V*) curve is quantified by a rectification ratio, defined as $R(V) = |I(V)/I(-V)|$. From Figure 2(a), it can be seen that each of these five configurations exhibits notable rectifying properties in a forward direction, meaning that the current is preferential to flow from the Pt to the Au end. Although the *I-V* curves share similar tendencies, they also demonstrate a nonlinear variation with molecular length. The current values of the molecular junction n = 3 are smaller than the others. With molecular length increasing (n > 3), the current values of the OPE molecular junctions improve, rather than decreasing, as might be expected (see Supplementary Information for more details)[26–28]. Also, the asymmetry of the current under positive and negative bias reduces as molecular length increases. That is to say, the rectification induced by asymmetric electrodes becomes less remarkable when the OPE molecule is extended.

To intuitively explore the nonlinear variation of current with molecular length, we use the current values and rectification ratios of the systems (n = 2 : 6) at 0.6 V bias as an representative example which is both typical and specific (see Supplementary Information for more details). From Figure 2(b), it can be seen that at 0.6 V bias, the molecular junction with n = 3 exhibits distinctive characteristics, having the lowest current and highest rectification ratio. As the number of benzene rings in the OPE molecule increases from 2 to 6, the current value drops at first and then rises, while its asymmetry varies inversely, with n = 3 as the inflection point.

The transmission of the configurations with n = 2 : 6 under 0.0 V bias is shown in Figure 3. This shows that for each junction, an electronic transmission spectrum exists near the Fermi energy level, leading to a notable increase in current within the low bias range. Since the transmission spectra close to the Fermi energy level play leading roles in electronic transport under nonzero bias voltage, we focus mainly on these. The transmission spectra of n = 3 are the most unfavorable to electronic transport compared with the others. With

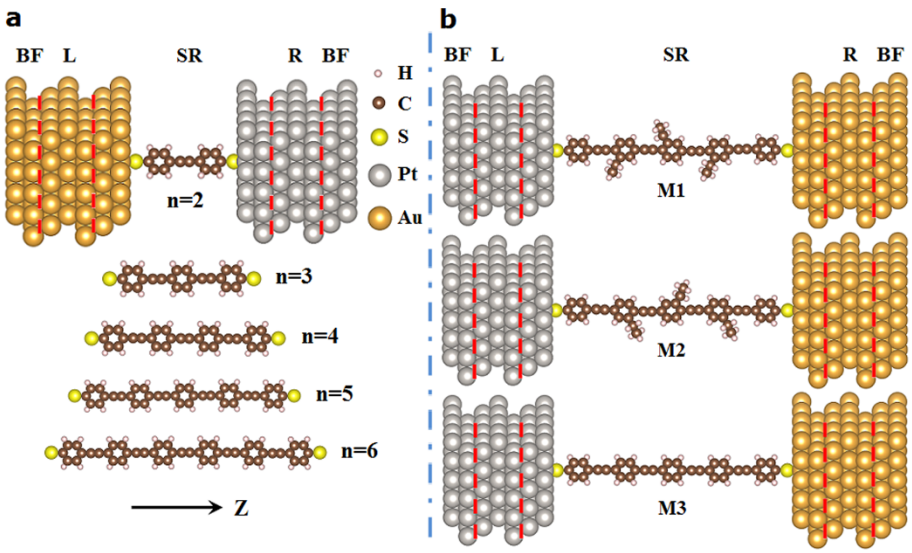

Figure 1 | Schematic structures of OPE heterometallic molecular junctions. (a) Models of different molecular length, containing 2–6 benzene rings (n = 2 : 6), with Au as the left electrode and Pt as the right electrode, respectively. (b) Models of the 5-benzene-ring OPE molecule; M1, the configuration reported in the experiment, M2, constructed by exchanging the OPE orientation (note that in both M1 and M2, the molecular core is the OPE with Et side groups), and M3, where the molecular core is replaced by the OPE without side groups. (SR: scattering region; L: left electrode; R: right electrode; BF: buffer layer).

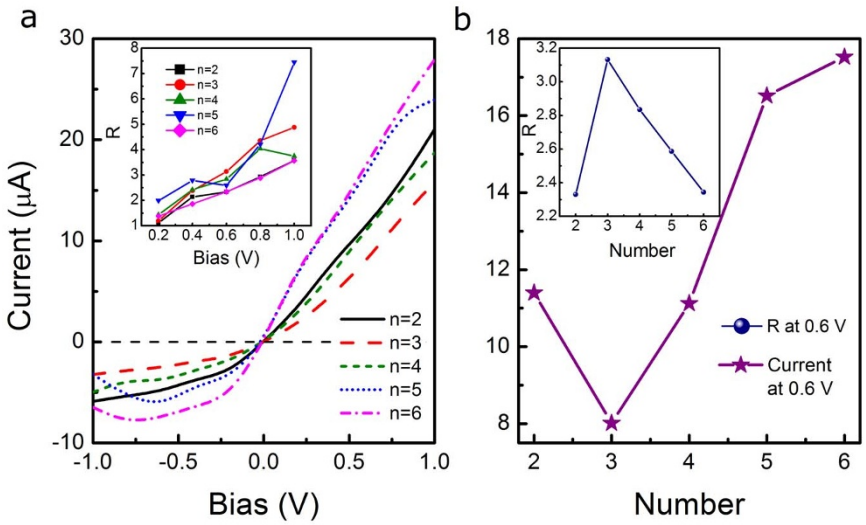

Figure 2 | Current properties of molecular junctions containing 2–6 benzene rings (n = 2 : 6) (a) *I-V* curves for each molecular junction. The inset shows the rectification ratios under bias. (b) Current value and rectification ratio for each molecular junction at 0.6 V bias. The horizontal ordinate indicates the number of benzene rings contained in the OPE molecular junctions.

the number of benzene rings in the OPE molecule ranging from 3 to 6, the spectra close to the Fermi energy level become more intense and delocalized, then more advantageous to conductance, similar to the trend seen in the currents. To clarify the contribution made by each part of the molecular junction to the transmission, we also investigate the OPE molecular eigenstates achieved by diagonalizing the molecular projected self-consistent Hamiltonian (MPSH) at 0.0 V bias voltage (note that the triangles in the figure indicate the eigenstates of bare molecular core). It is easily seen that, as molecular length increases, the highest occupied molecular orbital (HOMO) of the molecule shift to Fermi energy level, overlapping the existing peak nearby and resulting in higher current values for the longer molecular junctions. It is worth noting that the peaks near the Fermi energy level (denoted by A and B) correspond to no molecular eigenstates, meaning that the HOMO of molecule itself makes no contribution. Moreover, with increasing molecular length, the peak A firstly decreases and then increases with weakening delocalization, while the peak B declines and then disappears. By also calculating the MPSH of the extended molecule, which contains the molecule and the nearby atoms in the screening layers, we can verify that the peaks A and B are contributed by the coupling interaction between the molecule and the neighboring screening layer. For peak A, the coupling between the molecule and the nearest neighboring metal atoms contributes the most, while for peak B, the coupling between the molecule and the next nearest neighboring metal atoms plays a leading role. Therefore, we conclude that as molecular length increases, the coupling interaction between the molecule and the next nearest neighboring metal atoms in the screening layer weakens, converting to the former. Furthermore, with increasing length, the transmission shows more independent peaks contributed by molecular eigenstates; that is to say, the coupling interaction between molecule and electrode contributes less to the transmission with the share of molecular eigenstates holding the balance.

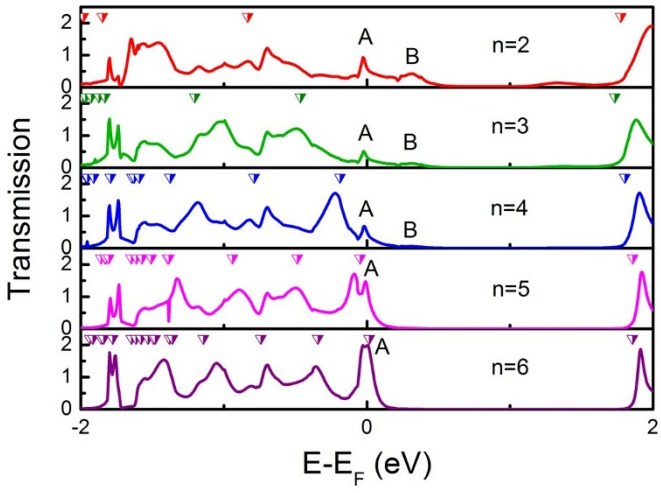

Figure 3 | **The transmission of molecular junctions (n = 2 : 6) shown in Figure 1(a) at 0.0 V bias.** The triangles indicate the MPSH eigenvalues of the OPE molecules. The uppercase letters A and B denote the two peaks near the Fermi energy level.

To clarify this point, we obtain the spatial distributions of the perturbed frontier molecular orbitals for the molecular junctions (n = 2 : 6) at 0.0 V bias voltage (see Table S1). From this analysis of Table S1, one can conclude that the current variation with molecular length is derived from the alteration of the molecular eigenstates and the coupling interaction between the molecule and electrodes induced by different molecular lengths.

Side group effect. The *I-V* curves of M1-3 are shown in Figure 4. At first glance, all three are similar, showing an inverse rectifying behavior owing to the exchange of electrodes compared to the configurations described in the previous section (as shown in Figure 1). However, it can be seen that there are certain differences between them. For example, for a current at ±1.0 V, the current of M1 at −1.0 V is about 22.6 μA, while that at 1.0 V is only 8.6 μA, leading to an inverted rectification (1/*R*) of 2.6. The *I-V* of M2, the configuration of which is obtained by exchanging the molecular orientation of M1 while keeping the electrodes unaltered, shows a higher inverse and lower forward current, with larger 1/*R*. This indicates that despite its asymmetric molecular structure, the rectifying behavior of M1 can be largely attributed to the asymmetric electrodes. To further determine the effect of the Et side group on the electronic transport of M1, we compare the *I-V* curves of M1 with M3. In contrast to the current of M3 in the respective ranges of bias, the Et side groups on M1 improve the current under the positive bias but suppress it under the negative one, resulting in a lower inverse rectification ratio. It can therefore be seen that although the Et side groups of M1 do not fundamentally change its rectifying properties, they do make a unfavorable

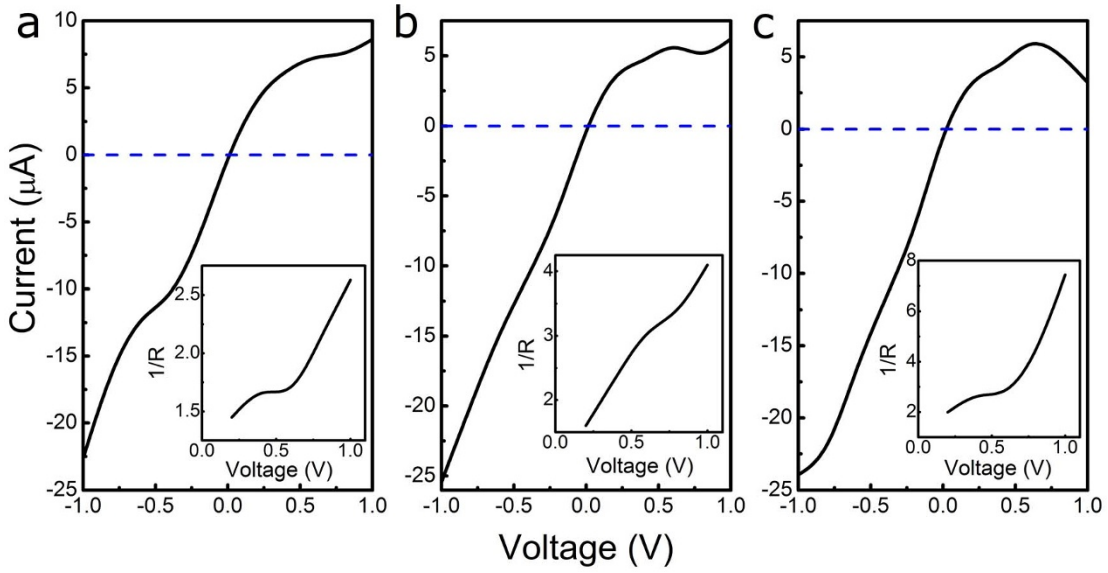

Figure 4 | *I-V* curves for molecular junctions: (a) M1, (b) M2, and (c) M3. The insets are the rectification ratios.

contribution to the rectification ratio. The effect of Et side groups on the spatial distributions of the frontier molecular orbitals of the OPE free molecule is shown in Table S2. It is worth noting that the rectification direction is different from that in Chen et al.'s experiment[23]. We attribute the discrepancy to the different sizes of electrodes surfaces in our theoretical simulation from that in experiment, according to our additional calculations of systems with electrodes of smaller sizes (see Figure S1). Our result predicts a possibility to design rectifiers with properties different from the experiment of Chen et al.[23] if the electrodes sizes are controlled to be small enough. Also, the current values of M1 are larger than the experimental ones. This can be attributed to the different configurations in our theoretical simulation from those in their experiment, as well as to the difference in the calculation methods (See Supplementary Information for more details).

Since the Et side group does not influence the electronic transport properties of M1 fundamentally, the following discussion focuses on explaining the mechanism of the rectifying properties of M1. Its electronic transmission spectra under different biases demonstrate that it has asymmetric current-voltage properties. From Figure 5, it can be seen that under 0.0 V bias voltage, there is an extensive and high electronic transmission spectrum close to the Fermi energy level, leading to a sharp increase of the current within the low bias range. With the application of a positive bias of 1.0 V, the transmission peaks shift out of the bias window and their expansibility decrease. However, with a negative voltage of −1.0 V, the transmission peaks close to E_F enter the bias window and make a contribution to the conductance. As a result, the current values at negative biases are larger than their positive counterparts. In addition, the electronic transmission spectra making a primary contribution to the conductance are mainly constituted by occupied molecular orbitals.

The asymmetric current-voltage properties can be understood by analyzing the MPSH eigenvalues. The triangles in Figure 5 denote these values for the extended molecular junction (including the molecular core and the 3 nearest metal atoms at each terminal) at the corresponding bias. It is obvious that the electron transport occurs mainly through the HOMO due to its proximity to the Fermi energy level. When a voltage is applied, the evolution of the HOMO is asymmetric. It moves far from the Fermi energy level at a positive bias and close to it at a negative bias. Moreover, HOMO-1 enters the bias window at −1.0 V. From this discussion, it is shown that the eigenvalues of the conducting channels decrease with the lowering Fermi energy levels of the right electrode, which occurs at a positive bias, and increase as it rises, which takes place at a negative bias. That is to say, the energy levels of the molecule contributing to the conductance can be markedly influenced by the variation of the Fermi energy levels of the right electrode. We can therefore deduce that the molecule couples more strongly with the right electrode; that is, the Au lead.

The modification of the wave function of the frontier orbitals at different biases can also help us to understand the mechanism of the rectifying properties of M1. Considering HOMO and HOMO-1 contribute mostly to electron transport; only these two orbitals are shown in Figure 5. At zero bias, the spatial distribution of the HOMO is slightly asymmetric, especially around the terminals, which is more delocalized at the right than the left end. This indicates that the molecule couples more intensely with the right electrode, verifying our previous inference. Applying a positive bias raises the Fermi energy level of the left electrode and depresses that of the right, injecting more electrons to the left side and depleting the electrons of the right side of the molecule. Thus, when a 1.0 V bias is applied, the

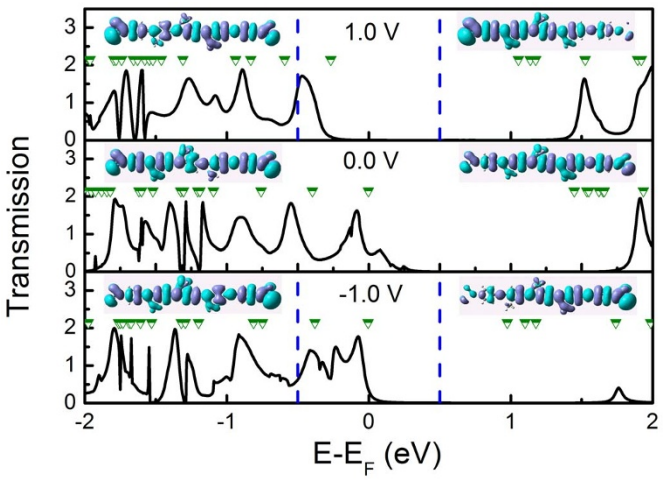

Figure 5 | Electronic transmission spectra and spatial distributions of the perturbed frontier molecular orbitals for M1 at different biases. The dashed lines indicate the bias windows for the transportation, and the triangles the MPSH eigenvalues. The molecular orbitals above the transmission spectra are the HOMO-1 (left) and HOMO (right), respectively.

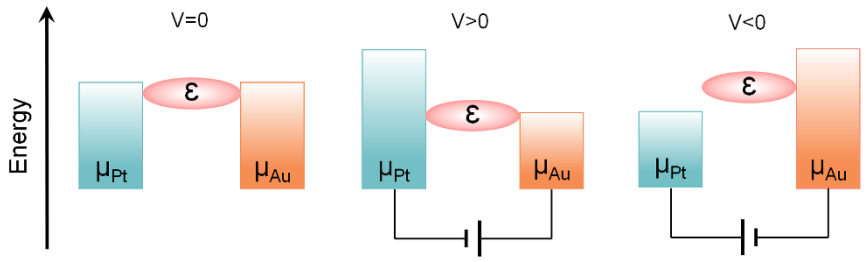

Figure 6 | Single-level models for the explanation of the electronic transport mechanism of M1.

HOMO becomes more localized to the left half, leading to a reduced coupling between the molecule and the right electrode, which is unfavorable to electron transport. Conversely, applying a −1.0 V bias results in the localization of the HOMO to the right side, which is also disadvantageous to electron transport. The entry of the delocalized HOMO-1 means that the current values at a negative bias are considerably larger than those at positive one.

The single energy level model offers a more concise summary of the electron transport in M1 (see Figure 6). At zero bias, the transport system is assumed to be in an equilibrium state. When a positive bias is applied, the Fermi energy level of the left electrode is lifted by eV/2, and that of the right is depressed by eV/2. Since the molecule couples more intensely with the right Au electrode, the conducting energy level of the molecule will decrease with the decline of the Fermi energy level of the right electrode, leading to a reduction in the scale of the orbitals in bias window, which reduces conductance. In contrast, when a negative bias is applied, the Fermi energy level of the right electrode is lifted by eV/2, and that of the left is depressed by eV/2. In this situation, the conducting energy level of the molecule will slightly increase rather than decrease, due to the elevated Fermi energy level. Consequently, increasing scales of orbitals will be included in the bias window, resulting in a conspicuous increase in current.

Figure 7 shows the potential drop along the transport direction of M1 with the bias of ±1.0 V applied. The structure of the molecular junction is shown in the background of the data. The dashed lines indicate the position of the terminal thiol groups, with the electrode regions lying outside of the lines and the molecular core within them. From the figure, it can be seen easily that the potential of the electrode layers close to the molecular core (the screening layers) fluctuates due to the influence of molecular potential. The potential of the layers further away from the molecular core tends to be invariable and smooth. With the bias of 1.0 V, the potential of the molecule drops dramatically and also fluctuates widely according to position. It is worth noting that a potential barrier or step occurs in the range [3.6, 5.0] nm, impeding the further access of electrons from the left to the right electrode. This is responsible for low current at positive bias. In the case of −1.0 V, the potential of the molecular core decreases sharply at first and then drops moderately from the right to the left side. The electrons from the right side encounter no distinct barrier, so can transfer from the high to the low potential effortlessly. The difference of potential drops at 1.0 V and −1.0 V is enough to induce a rectification of 2.5 at this bias. This is also consistent with the wave function of the frontier orbitals. At 1.0 V bias, the HOMO is localized at the left side of the molecular junction, which plays a dominant role in electronic transport, resulting in a potential barrier on the right side. At −1.0 V bias, although the HOMO is localized at the right side, the HOMO-1 is delocalized over the entire molecular junction. This also contributes to electronic transport, leading to an overlapping interaction with the HOMO, and so there is no significant potential barrier at −1.0 V. Moreover, it can also be related to the single level model in Figure 6. At 1.0 V, the potential across the right side of the molecule is close to the potential of Au lead, while for the left side of the molecule, the potential drops dramatically, showing that the potential on the molecule is affected more by that on the right Au electrode. This is another indication of a stronger coupling and a closer electron exchange between the OPE molecule and the Au lead. However, at the bias of −1.0 V, the molecular energy level lies between the Fermi levels of the Pt and Au (as shown in Figure 6), so does the molecular potential, which drops almost smoothly from high to low one at −1.0 V.

Discussion

By analyzing the charge distribution on the molecular junction, we find that the left Pt electrode and the molecular core are negatively charged, denoting an excess of electrons, while the right Au electrode is positively charged, indicating a lack of them. As for M1, the HOMOs play a leading role in electronic transport, meaning that the "hole" is the carrier of the current. Thus, the OPE can be considered as a p-type semiconductor. The Schottky contacts between the metal electrodes and the p-type semiconductor-like OPE molecule before and after contact are shown in Figure 8. The Fermi energy level of Au is the highest, followed by Pt, with OPE molecular last, meaning that it has the strongest electronegativity. Once they come into contact with each other, the Au electrode provides electrons to the OPE molecule and Pt electrode to reach an equilibrium state. After the equivalent Fermi energy level has been achieved, the Pt electrode obtains some electrons and OPE obtains still more. Consequently, a large barrier appears at the contact region of the molecule and Au electrode, which is disadvantageous to conductance. Compared to this aspect, the barrier at the contact region of the molecule and Pt electrode can be neglected, generating asymmetric Schottky contact barriers at these two contacts of the molecule, which is the root cause of the rectification. This can also be understood in the case of the voltage drop at the biases in Figure 7. When a

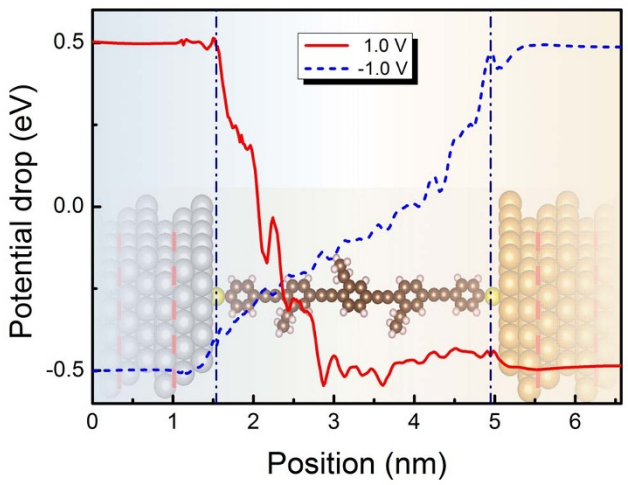

Figure 7 | Potential drop along the transport direction of M1 with ±1.0 V bias applied. The dashed lines indicate the position of the S atom in the z-axis. The background of the data shows the structure of the molecular junction.

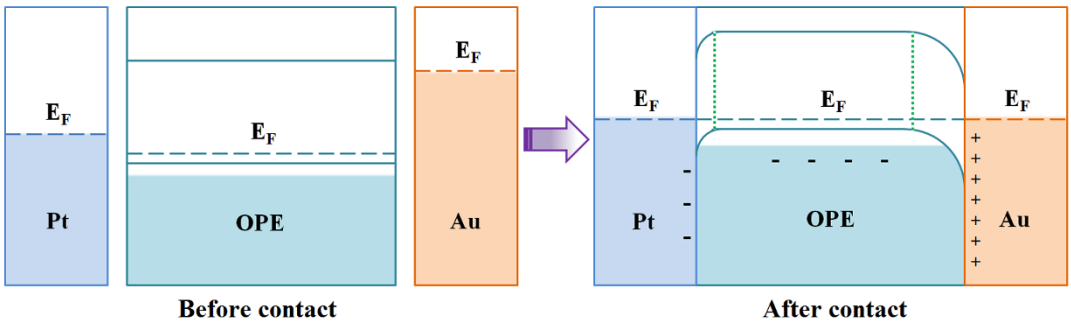

Figure 8 | Schematic diagram of the Schottky contact between a p-type semiconductor-like molecule with metals. The regions between the metal edges and the green dotted lines are the depletion layers.

bias of −1.0 V bias is applied, the Fermi energy level of Au is lifted and that of Pt is depressed, leading to a narrower depletion layer at each contact region. Accordingly, the electrons can surpass the barrier easily to transfer from the right side to the left. However, with the voltage of 1.0 V applied, the depletion layers broaden further, especially at the OPE-Au contact region, making it significantly harder for electrons with low energy at that position to tunnel. Thus, in this situation, rectifying behavior emerges. In addition, after the formation of a junction, the Fermi energy level of the OPE molecule and Pt electrodes will undoubtedly rise, as shown in Figure 8.

In summary, by applying quantum transport calculations based on first principles theory, we have theoretically investigated the rectifying behavior of an α,ω-dithiol terminated OPE molecule sandwiched between Pt and Au electrodes exhibiting molecular length and side group effects. Our results show that when the molecule lengthens, the currents of the molecular junctions vary nonlinearly. As the number of benzene rings in the OPE increases from 2 to 6, the one containing 3 rings shows the highest rectification ratio and lowest current. The current increases with molecular length while its asymmetry reduces. This variation is derived from the difference in molecular eigenstates and the coupling between the molecule and electrodes induced by the varying molecular length. The Et side group does not fundamentally influence the electronic transport properties of the molecular junction, but hinders the achievement of high rectification of the OPE molecular junction. The rectifying behavior of heterometallic molecular junctions can be attributed to the asymmetric contacts between the molecule and different metal electrodes, which leads to asymmetric Schottky barriers being formed at contact regions. This analysis provides a fundamental understanding of the rectification induced by asymmetric electrodes, and predicts that rectifiers with different rectification direction from those in the previous experiment can be designed, according to the size effect of electrodes.

Methods

The entire molecular junction is divided into three regions; a left electrode, a scattering region, and a right electrode. The two metal layers outside the electrodes are buffer layers, which are necessary to create a bulk environment for the heterometallic electrodes. Two layers of metal atoms in each electrode and the molecule constitute the scattering region, which is optimized by the SIESTA package[29] with a maximum force of 0.02 eV/Å. During the optimization, the anchoring atoms are only allowed to relax along the transport direction and the relative positions of the electrode surface layers are frozen except for the distance between the two electrodes. Each semi-infinite gold electrode is simulated by a $5 \times 5 \times 3$ unit cell. Due to the nonconformity of the lattice constant of heterometallic electrodes, the models are dealt with by imposing nonperiodic boundary conditions; that is, $1 \times 1 \times 1$ k-points are chosen in the xyz direction. We employ the improved Troullier-Martins type norm-conserving pseudopotentials to describe the core electrons and linear combinations of the atomic orbitals to expand the valence states of electrons. The Perdew-Burke-Ernzerhof (PBE) formulation for the generalized gradient approximation (GGA) is adopted for the exchange-correlation functional, which generally performs better for molecules and metals. Although the PBE-GGA usually overestimates the HOMO level and underestimates the HOMO-LUMO gap of molecules while describe the band structure of metals well, the theoretical studies show that the PBE-GGA usually provides satisfying results for the description and explanation of the trend of experimental phenomena rather than the magnitudes of values. In all the calculations a single-ζ plus single polarization (SZP) basis set is employed for the metal atoms and a double-ζ plus single polarization (DZP) basis for the other atoms. We note that the SZP is comparable with even higher level basis set[30] in calculations involving metal atoms as we conduct in this work to obtain reliable results that can reveal the trends of key physical quantities and to understand the underlying mechanisms.

Current through the junctions is calculated by the Landauer-Büttiker formula:

$$I = \frac{2e}{h}\int T(E,V)[f(E-\mu_L)-f(E-\mu_R)]dE$$

where e is the electron charge, h is Planck's constant, and $T(E,V)$ is the transmission function of the junctions at energy E under the bias voltage V. $f(E-\mu_L)$ is the Fermi-Dirac distribution function with the electrochemical potential $\mu_{L/R}$ of the left (right) electrode. The electronic transport properties are calculated using the ab initio code TranSIESTA[31].

1. Aviram, A. & Ratner, M. A. Molecular Rectifiers. *Chem. Phys. Lett.* **29**, 277–283 (1974).
2. Reed, M. A. *et al.* Conductance of a Molecular Junction. *Science* **278**, no. 5336, 252–254 (1997).
3. Kiguchi, M. *et al.* Conductance of single 1,4-disubstituted benzene molecules anchored to Pt electrodes. *Appl. Phys. Lett.* **91**, 053110 (2007).
4. Ng, M.-K. *et al.* Molecular Diodes Based on Conjugated Diblock Co-oligomers. *J. Am. Chem. Soc.* **124**, 11862–11863 (2002).
5. Elbing, M. *et al.* A single-molecule diode. *PNAS* **102**, 8815–8820 (2005).
6. Gasyna, Z. L. *et al.* Asymmetric current–voltage characteristics of molecular junctions containing bipolar molecules. *Chem. Phys. Lett.* **417**, 401–405 (2005).
7. Morales, G. M. *et al.* Inversion of the Rectifying Effect in Diblock Molecular Diodes by Protonation. *J. Am. Chem. Soc.* **127**, 10456–10457 (2005).
8. Díez-Pérez, I. *et al.* Rectification and stability of a single molecular diode with controlled orientation. *Nature Chem.* **1**, 635–641 (2009).
9. Huang, J. *et al.* Rectifying Effect in Polar Conjugated Molecular Junctions: A First-Principles Study. *J. Nanosci. Nanotechnol.* **9**, 774–778 (2009).
10. Zhang, Z. *et al.* All-carbon sp-sp2 hybrid structures: Geometrical properties, current rectification, and current amplification. *Sci. Rep.* **3**, 2575 (2013).
11. Hu, G. C. *et al.* Length-dependent inversion of rectification in diblock co-oligomer diodes. *Appl. Phys. Lett.* **99**, 082105 (2011).
12. Deng, X. *et al.* Length and end group dependence of the electronic transport properties in carbon atomic molecular wires. *J. Chem. Phys.* **132**, 124107 (2010).
13. Lee, Y. *et al.* Understanding the Anchoring Group Effect of Molecular Diodes on Rectification. *Langmuir* **25**, 1495–1499 (2009).
14. Zhang, G.-P. *et al.* Modulation of Rectification in Diblock Co-oligomer Diodes by Adjusting Anchoring Groups for Both Symmetric and Asymmetric Electrodes. *J. Phys. Chem. C* **116**, 22009–22014 (2012).
15. Li, Z. & Kosov, D. S. Orbital Interaction Mechanisms of Conductance Enhancement and Rectificaiton by Dithiocarboxylate Anchoring Group. *J. Phys. Chem. B* **110**, 19116–19120 (2006).
16. Zhang, G. P. *et al.* Effect of contact configurations on the rectification of dipyrimidinyl-diphenyl diblock molecular junctions. *Chin. Phys. B* **20**, 127304 (2011).
17. Zhao, J. *et al.* Molecular Rectificaiton Based on Asymmetrical Molecule-Electrode Contact. *J. Phys. Chem. C* **114**, 4135–4141 (2010).
18. Nakamura, H. *et al.* Switch of Conducting Orbital by Bias-Induced Electronic Contact Asymmetry in a Bipyrimidinyl-biphenyl Diblock Molecule: Mechanism to Achieve a pn Directional Molecular Diode. *J. Phys. Chem. C* **115**, 19931–19938 (2011).
19. Li, Z. *et al.* Protonation effects on electron transport through diblock molecular junctions: A theoretical study. *Sci. China Ser. B-Chem.* **51**, 1159–1165 (2008).
20. Zhang, G.-P. *et al.* Theoretical Studies on Protonation-Induced Inversion of the Rectifying Direction in Dipyrimidinyl−Diphenyl Diblock Molecular Junctions. *J. Phys. Chem. C* **116**, 3773–3778 (2012).

21. Kostyrko, T. *et al*. Current rectification in molecular juncions produced by local potential fields. *Phys. Rev. B* **81**, 085308 (2010).
22. Deshmukh, M. M. *et al*. Fabrication of Asymmetric Electrode Pairs with Nanometer Separation Made of Two Distinct Metals. *Nano Lett.* **3**, 1383–1385 (2003).
23. Chen, X. *et al*. Chemical Fabrication of Heterometallic Nanogaps for Molecular Transport Junctions. *Nano Lett.* **9**, 3974–3979 (2009).
24. Pan, J. B. *et al*. Current rectification induced by asymmetrical electrode materials in a molecular device. *Appl. Phys. Lett.* **98**, 092102 (2011).
25. Fang, C. *et al*. Effect of different electrodes on Fano resonance in molecular devices. *Appl. Phys. Lett.* **100**, 023303 (2012).
26. Peng, G. *et al*. Conductance of Conjugated Molecular Wires: Length Dependence, Anchoring Groups, and Band Alignment. *J. Phys. Chem. C* **113**, 20967–20973 (2009).
27. Visontai, D. *et al*. Electron transport through ribbonlike molecular wires calculated using density-functional theoryand Green's function formalism. *Phys. Rev. B* **81**, 035409 (2010).
28. Koch, M. *et al*. Voltage-dependent conductance of a single graphene nanoribbon. *Nature nanotechnology* **7**, 713–717 (2012).
29. Sánchez-Portal, D. *et al*. Density-Functional Method for Very Large Systems with LCAO Basis Sets. *Int. J. Quantum Chem.* **65**, 453–461 (1997).
30. García-Gil, S. *et al*. Optimal strictly localized basis sets for noble metal surfaces. *Phys. Rev. B* **79**, 075441 (2009).
31. Brandbyge, M. *et al*. Density-functional method for nonequilibrium electron transport. *Phys. Rev. B* **65**, 165401 (2002).

Acknowledgments

The work described in this paper is supported by a grant from the Research Grants Council of Hong Kong SAR [project No. CityU 103812].

Author contributions

X.X.F. performed all the calculations. X.X.F. and R.Q.Z. contributed the ideas, the data analysis and the writing of the manuscript. G.P.Z. and Z.L.L. discussed some details with the first author.

Additional information

Supplementary information accompanies this paper at http://www.nature.com/scientificreports

Competing financial interests: The authors declare no competing financial interests.

How to cite this article: Fu, X.-X., Zhang, R.-Q., Zhang, G.-P. & Li, Z.-L. Rectifying Properties of Oligo(Phenylene Ethynylene) Heterometallic Molecular Junctions: Molecular Length and Side Group Effects. *Sci. Rep.* **4**, 6357; DOI:10.1038/srep06357 (2014).

This work is licensed under a Creative Commons Attribution-NonCommercial-NoDerivs 4.0 International License. The images or other third party material in this article are included in the article's Creative Commons license, unless indicated otherwise in the credit line; if the material is not included under the Creative Commons license, users will need to obtain permission from the license holder in order to reproduce the material. To view a copy of this license, visit http://creativecommons.org/licenses/by-nc-nd/4.0/